Shell corrections in stopping powers

H. Bichsel*
Center for Experimental Nuclear Physics and Astrophysics, Box 354290, University of Washington, Seattle, Washington 98195-4290
(Received 28 June 2001; published 24 April 2002)

One of the theories of the electronic stopping power S for fast light ions was derived by Bethe. The algorithm currently used for the calculation of S includes terms known as the mean excitation energy I, the shell correction, the Barkas correction, and the Bloch correction. These terms are described here. For the calculation of the shell corrections an atomic model is used, which is more realistic than the hydrogenic approximation used so far. A comparison is made with similar calculations in which the local plasma approximation is utilized. Close agreement with the experimental data for protons with energies from 0.3 to 10 MeV traversing Al and Si is found without the need for adjustable parameters for the shell corrections.

DOI: 10.1103/PhysRevA.65.052709 PACS number(s): 34.50.Bw

I. INTRODUCTION

An important concept in the description of the interactions of fast charged particles with matter is the stopping power $S=-dT/dx$. It gives the average energy loss per unit path length of the particles, and is used in applications such as nuclear physics, radiation detectors, cancer therapy, space exploration, etc. Reviews can be found in Bohr [1], Fano [2], NAS-NRC Publication 1133 [3], Inokuti [4], ICRU report 49 [5], Bichsel [6–8], and Ziegler [9]. The theory considered here was developed by Bethe [10–12], Bloch [13], and others [14,15]. The present study describes the functions needed for the calculation of S for practical applications, and is restricted to protons and α-particles with nonrelativistic speeds. An important aspect is the comparison with the experimental measurements. The expression used to calculate S is given in Sec. II with short descriptions of its components. In Sec. III, the principal parts of the study, the calculations of the stopping number B and the shell corrections C, are given. The emphasis is on the numerical determination of B and C rather than a derivation with theoretical-analytical methods. Calculations are made with a model more realistic than the hydrogenic approximation [5]. Since these calculations are complex, results for Al and Si only are given. A comparison with other models is made.

In experimental measurements, the energy loss (straggling) spectra $\phi(x,T,T_1)$ (where T is the initial energy of the particle, and T_1 is its energy after traversing an absorber of thickness x) are measured. A discussion of the measurements and use of S is given in Sec. IV. Finally, experimental data of shell corrections are compared with the present calculations in Sec. V.

Note that, for thin absorbers, the mean energy loss loses its usefulness, and a more appropriate quantity is the most probable energy loss [8,16–18]. A description of the physical processes in the energy-loss interactions can also be found, e.g., in Refs. [7,8,19].

The calculations are presented from an experimental point of view, viz., particle speed is represented by the kinetic energy of the particles, stopping numbers are given for specific elements. The present theory gives calculations of S with no free parameters for the shell corrections, and is accurate to about $\pm 0.4\%$ for $T>10$ MeV, about 1% at $T=0.5$ MeV.

II. CALCULATION OF STOPPING POWER

Discussions of the Bethe theory of S can be found in many papers [2–4,6]. Here, the formulation given in Refs. [5,20,21] is used. The mass stopping power S (in MeV cm^2/g) of particles with charge ze, kinetic energy T, and speed $v=\beta c$ is calculated with

$$S=-\frac{dT}{dx}=\frac{2\pi e^4}{mc^2}\frac{z^2}{\beta^2}nB=\frac{kz^2}{\beta^2}nB=\frac{0.15354}{\beta^2}\frac{z^2Z}{A}B, \tag{1}$$

where $mc^2=510.999$ keV is the rest mass of an electron, $k=2.54955\times10^{-19}$ (eV cm^2) [8], $n=6.0221\times10^{23}Z/A$ the number of electrons per gram, Z and A (g) the atomic number and weight of the absorber, and B is the dimensionless ''stopping number.'' Other parameters used are the proton mass $Mc^2=938.256$ MeV, and, for Al $Z=13$, $A=26.9815$ g/mole, for Si $Z=14$, $A=28.086$ g/mole.

Bethe [10] derived an approximation for B given by $B_a=2L_a$,

$$L_a(\beta)=\ln\frac{2mc^2\beta^2\gamma^2}{I}-\beta^2\equiv f(\beta)-\ln I\sim\ln 2mv^2/I, \tag{2}$$

where $\gamma^2=1/(1-\beta^2)$ [22], I is the mean excitation energy of the electrons in the atom, and the last expression is the nonrelativistic approximation.

A better approximation is obtained with

$$L(\beta)=L_a(\beta)-\frac{C(\beta)}{Z}+zL_1(\beta)+L_2(z,\beta), \tag{3}$$

where $C(\beta)$ is the sum of shell corrections and L_1 and L_2 are the Barkas and Bloch correction terms. These functions

*Author to whom correspondence should be addressed. 1211 22nd Avenue East, Seattle, WA 98112-3534. FAX: 206-685-4634. Email address: bichsel@npl.washington.edu

TABLE I. Values of functions occurring in Eqs. (2) and (3) for protons with energy T (MeV) traversing Al, $I=166$ eV, $\ln I=5.112$. The Bethe asymptotic stopping number, Eqs. (2) and (15), is $L_a(\beta)=f(\beta)-\ln I$, the Bethe approximation for the stopping number, Eq. (14), is $L_b= L_a-\Sigma C_i/Z$, with C_i according to Sec. III C; the stopping number including the corrections discussed in Sec. II B and Sec. II C is $L=L_b+zL_1+L_2(z)$, Eq. (3). The last column gives the ratio r of $\Sigma C_i/Z$ to L, in percent.

T	β^2	$f(\beta)$	L_a	L_b	L	C_K/Z	C_L/Z	C_M/Z	L_1	$-L_2$	r
0.3	0.00064	6.482	1.370	1.234	1.374	−0.1568	0.2731	0.0201	0.2343	0.0935	9.9
1.0	0.00213	7.685	2.573	2.349	2.461	−0.0111	0.2282	0.0070	0.1418	0.0295	9.1
3.0	0.00636	8.780	3.668	3.493	3.544	0.0694	0.1032	0.0023	0.0607	0.0100	4.9
10	0.02098	9.973	4.861	4.771	4.786	0.0565	0.0328	0.0007	0.0176	0.0030	1.9
30	0.06101	11.043	5.931	5.896	5.900	0.0241	0.0106	0.0002	0.0051	0.0010	0.6

(except L_2) depend on Z. Values for the functions in Eq. (3) are given in Table I. Some further corrections are mentioned in Sec. II D. Several terms in Eqs. (2) and (3) are considered next, while the Bethe derivation of B and the shell correction C are discussed in Sec. III.

A. *I* values

The mean excitation energy I can be calculated from

$$\ln I=\int f(E,0)\ln E\,dE \Big/ \int f(E,0)dE, \tag{4}$$

where $f(E,0)$ is the dipole oscillator strength for an energy transfer E and $f(E,0)$ is closely related to the optical absorption coefficients [10,2,4]. A derivation of $\ln I$ is given in Sec. III A. For Al, a value $I=165.7$ eV has been calculated with Eq. (4) [23]. This value agrees with $I=167$ eV, derived from the measurements for protons with energies from 12 to 30 MeV [24]. Here, $I=166$ eV is used. For Si, $I=173.5$ eV was measured in Ref. [24], while $I=176$ eV was found from measurements with 70 MeV protons [25]. The value $I=173.5$ eV is used here, and energy-loss measurements with 290 MeV/u C ions [26] and measurements of straggling in Ref. [17] agree with this value. An uncertainty of ± 2 eV should be assumed for the I values.

B. Bloch correction

Lindhard and Sørensen [27,28] showed that the correction term

$$L_2=-y^2\sum_{l=1}^{\infty}\frac{1}{l(l^2+y^2)}, \tag{5}$$

with $y=zv_0/v=\alpha z/\beta=z/(137\beta)$,[1] is caused by a difference in the perturbation and exact transport cross sections. This function was originally described by Bloch [13], and a simple description was given in Ref. [29]. It originates from close collisions of the ions and the target electrons and is here assumed to depend little on the absorber. The function L_2 is used without the scaling factor introduced in Ref. [30], see Fig. 7 in Ref. [31]. Note that L_2 is proportional to z^2 only for small y, where $L_2\sim -1.202y^2$, see Table I.

C. Barkas correction

In a classical description of the collisions [32–34] the Barkas effect arises from the inclusion of the displacements of electrons from their equilibrium positions during the collision. Since no complete theory of L_1 is available, an empirical approach is used here. A function L_1, derived by Ashley, Ritchie, and Brandt [33], based on the harmonic-oscillator model, is used to approximate the Barkas correction [31]. It is given by

$$L_1=\frac{\gamma F(b/x^{1/2})}{Z^{1/2}x^{3/2}}, \tag{6}$$

where $x=v^2/(Zv_0^2)=18779\beta^2/Z$, and b and γ are the parameters fitted to the experimental data. Note that L_1 does not depend on particle mass or charge.

In Eq. (10) of Bichsel [31] it is seen that the experimental values of L_1 can be determined from the measurements for protons and α particles with the same speed if it is assumed that C/Z does not depend on particle mass and charge. Similarly, Eq. (12) of Ref. [31] gives experimental values of L_1 for particles and antiparticles. From a least-squares fit with Eq. (6) to the experimental data for Al of Andersen *et al.* [30] the parameters $\gamma=2.04, b=1.78$ were found. For the experimental data of Andersen *et al.* [35] for protons and antiprotons in Si, the values $\gamma=2.04, b=1.88$ gave a good fit.

From the uncertainty (± 0.003) of Δ_{He} given in Ref. [30], the uncertainty of L_1 is ± 0.007 at 0.8 MeV, increasing to ± 0.0126 at 5.6 MeV/nucleon. This uncertainty will enter directly into the calculation of experimental shell corrections, Sec. V A, but will be the same for all experimental data. The use of Eq. (6) for energies below 0.8 MeV/u and above 5.6 MeV is an extrapolation which may give unreliable results.

Since L_1 here is a function derived from the experimental data for protons and α particles, a number of effects discussed in Ref. [34] (e.g., angular deflections of the particles during energy losses to electrons, assumptions about the atomic model used in Refs. [33,36]) are lumped into the approximation for L_1. The dependence on particle charge appears only in the coefficient z of L_1 in Eq. (3). Thus the

[1] $v_0=\alpha c$ is the Bohr velocity.

use in Eq. (6) of different b for protons and α particles by Porter (e.g., Ref. [37]) is inconsistent with the basic concept of the Barkas correction. While the parameters b and γ are not derived from first principles, they are not adjustable for the present comparison with the experimental data.

D. Other corrections

A number of corrections have been discussed by Ahlen [38] and by Lindhard and Sørensen [27]. They are important for fast, heavy ions (e.g., C, Fe) and would have to be included in Eq. (3). For the particles and speeds considered here, these corrections are small; the largest one among them is the ''nuclear stopping power'' [5], and yet it contributes less than 0.1% above 0.4 MeV/u. The close collision Mott correction $G(z,\beta)$, Eq. (4.23) of [38] amounts to 0.03% of B for 30 MeV protons, and increases with $z\beta$—it might amount to the order of 2% for 300 MeV/u Fe ions. The electron capture and loss effects should be very small for protons with energies above 0.3 MeV [39]. For α particles, see Sec. V C, and for Li ions, see Table II in Ref. [31]. A correction due to the polarization of the medium is the density effect δ [5,8,22,40,41]. It amounts to 6×10^{-5} of B at 30 MeV. The effect of multiple scattering must be considered in the experimental measurements [3,42–44], see Sec. IV.

III. STOPPING NUMBER B AND SHELL CORRECTIONS C

In this section methods used to calculate B are described. In Secs. III A, III B, and III C, Bethe's quantum-mechanical calculation with the first Born approximation of the collision cross sections, and in Sec. III D, the Lindhard-Winther [45] method giving the interaction with a free-electron gas are described. The harmonic-oscillator model is not considered here; it was used in the description of the Barkas effect in Sec. II C and was discussed by Sigmund and Haagerup [46]. Another method used to obtain B is a scaling procedure, Sec. III E.

A. The Bethe calculation

In the first Born approximation, for nonrelativistic speeds, Livingston and Bethe [12] gave the stopping number B as

$$B(v)=\int dE\int_{Q_m}^{\infty} f(E,Q)\,dQ/Q, \tag{7}$$

where $f(E,Q)$ is the generalized oscillator strength (GOS [4]) for a transition from the ground state of the atom to an excited state of energy E, $Q=K^2/2m$ represents the (hypothetical) recoil energy resulting from the momentum transfer K from the incident particle to a free electron, and $Q_m=E^2/2mv^2$ (for a more exact expression for Q_m, see Inokuti [4]). The calculation of B can be made for each atomic shell separately [47].

In order to avoid explicit calculations of $f(E,Q)$, Bethe [10] used the following approach that is valid only for the whole atom. He divided the integral over Q into three parts:

$$B(v)=\int dE\left\{\int_{Q_m}^{Q_1} f(E,0)\,dQ/Q+\int_{Q_1}^{\infty} f(E,Q)\,dQ/Q+\int_{Q_m}^{Q_1}[f(E,Q)-f(E,0)]\,dQ/Q\right\}, \tag{8}$$

where Q_1 is a small, fixed value. The integral of the first part is

$$B_1(v)=\int dE\, f(E,0)\int_{Q_m}^{Q_1} dQ/Q$$

$$=\int dE\, f(E,0)\ln\frac{Q_1}{(E^2/2mv^2)} \tag{9}$$

$$=\ln 2mv^2Q_1-\int dE\, f(E,0)\,2\ln E=\ln\frac{2mv^2Q_1}{I^2}, \tag{10}$$

where the sum rule

$$\int f(E,0)\,dE=1 \tag{11}$$

for the dipole oscillator strength $f(E,0)$ was used for the first term of Eq. (10) and the logarithmic mean excitation energy $\ln I$ already defined in Eq. (4) is obtained from the second term.

For the second part, B_2, the order of integration is exchanged and the upper limit ∞ in the integral over Q is replaced by $Q_M=2mv^2$ (see Figs. 3 in Refs. [2] and [45]), resulting in

$$B_2(v)=\int_{Q_1}^{2mv^2}\frac{dQ}{Q}\int dE\, f(E,Q). \tag{12}$$

With the sum rule for the generalized oscillator strength

$$\int f(E,Q)\,dE=1, \tag{13}$$

we get

$$B_2(v)=\ln\frac{2mv^2}{Q_1}. \tag{14}$$

If we assume for the third part B_3 that v is large, Q_m can be replaced by zero, and the integral is equal to zero because of the sum rule, Eq. (13), then the Bethe asymptotic stopping number is[2]

$$B_a(v)=B_1(v)+B_2(v)=\ln\frac{(2mv^2)^2}{I^2}=2L_a. \tag{15}$$

The errors in this derivation of Eq. (15) can be corrected by defining the Bethe approximation [12]

[2]The factor 2 in Eq. (15) frequently is included with the coefficient 0.153 54 in Eq. (1), giving a coefficient of 0.307 08.

$$L_b = L_a - C/Z. \tag{16}$$

Values of L_a and L_b are given in Table I. Equation (53) of Fano [2] shows that C/Z consists of two parts, viz., $C = C_1 + C_2$, where

$$C_1 = \frac{1}{2}\int dE \int_0^{Q_m} [f(E,Q) - f(E,0)] \frac{dQ}{Q} \tag{17}$$

corrects for setting $Q_m = 0$ in B_3, and

$$C_2 = -\frac{1}{2}\int dE \int_{2mv^2}^{\infty} f(E,Q) \frac{dQ}{Q} \tag{18}$$

corrects for the changes made with Eqs. (12) and (13), see Figs. 2 and 3 in Ref. [2]. The correction can be calculated separately for each atomic shell. Corresponding corrections for the electron-gas model are illustrated in Fig. 3 of Lindhard and Winther [45].

The correction C is due to the approximations made in deriving Eq. (15) and is only indirectly related to the orbital speeds of the electrons in the atoms. No formal name for $C(v)$ was used in the Bethe-Walske papers [12,14]. To the extent that C is calculated for each atomic shell, the expression ''shell correction'' makes sense and it was used with this meaning in Ref. [48]. Note also that the correction needs to be made for *all* shells [45], and the expression ''inner shell corrections'' is an approximation implying that the corrections for outer shells can be neglected. The first calculations of $C_K(v)$ for K shell electrons were given in Refs. [12,14].

B. Calculation of $f(E,Q)$, B and C with hydrogenic wave functions

If Coulomb wave functions are used to represent electrons ejected from atoms, analytic expressions can be derived for the generalized oscillator strength $f(E,Q)$. Such functions may be found in Refs. [12,14,49]. Calculations of stopping number B and shell corrections C with these functions were made for K- and L-shell electrons by Walske [14] and for M shell electrons by Bichsel [50]. Walske suggested that the L shell results would not be accurate for atoms with $Z < 30$. This can be seen in Fig. 1, where C_L calculated for Si is shown. These results were obtained with numerical integrations that pose problems for the accuracy of the results described in Ref. [50]. Similar problems occur for the calculations described in the following section.

C. Calculation of $f(E,Q)$, B and C with Hartree-Slater wave functions

Calculations of $f(E,Q)$ were made with the method described by Manson [51]. For the ground-state wave functions and the atomic potentials data from the Herman-Skillman tables [52] were used. They were calculated with the Hartree-Slater approximation. Wave functions for electrons in continuum states were calculated by numerical integration of the Schrödinger equation as described by Manson [51]. Such calculations were made for the K shell and both L subshells for Al and Si for 320 excitation energies E between 0 and 2500 Ry, and for more than 1000 values of Q. Specifically, Q was increased until $f(E,Q_l)$ was less than 10^{-5} of $\int^{Q_l} f(E,Q)\, d \ln Q$. Typically, Q_l was about $2E$ or $3E$, with the maximum value of $f(E,Q)$ occurring at $Q \sim E$ (''Bethe ridge'' [4]). In order to check the accuracy of the numerical integrations over E, the tables of $f(E,Q)$ are extended by cubic spline interpolation [53] for up to 2000 values. The stopping numbers B were calculated with Eq. (7) and the shell corrections with Eqs. (17) and (18). Results for C_K and $C_L = C_{2s} + C_{2p}$ are shown in Fig. 1 for Si. For the M shell electrons, this approach cannot be used because the M electrons are shared in the solid-state structure of the materials. Therefore, these electrons are considered as an electron gas with the stopping number $B = 2L$ given by Lindhard and Winther in Fig. 4 of Ref. [45]. The first correction term in Eq. (20) of Ref. [45] is used as an approximation

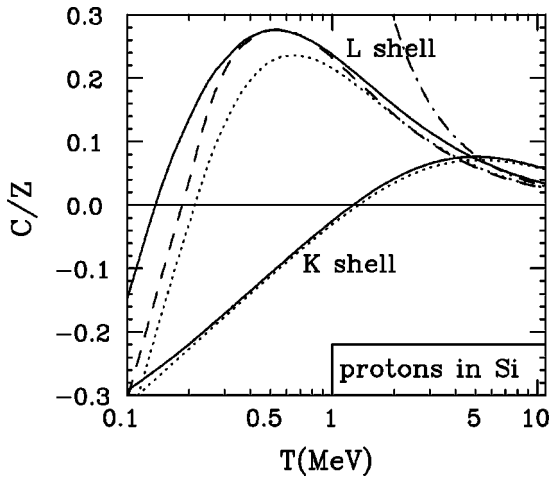

FIG. 1. K- and L-shell corrections for Si ($Z = 14$) as a function of proton energy T. The solid lines show C_K and $C_L = C_{2s} + C_{2p}$ calculated with the present theory. The dotted lines are C_K and C_L calculated with the hydrogenic approximation of Sec. III B with the canonical parameters given by Walske [14] (viz., $Z_{Leff} = Z - 4.15$ and $\Theta_L = 0.35$). A function to match C_L at the peak, shown by the dashed line, was calculated with the scaling method, Eq. (22), with $V_L = 1.17$, $H_L = 1.2$. The dash-dotted line gives the approximation defined by Eq. (21).

$$C_M = \frac{0.3 m v_F^2}{m v^2/2} Z = a_M / T, \tag{19}$$

where v_F is the Fermi speed, T (MeV) is the energy of a proton, and a_M is a constant. For Al, $a_M = 0.090$ MeV, and for Si, $a_M = 0.109$ MeV. Fano [2,3] gave an equivalent expression in his Eq. (58). The contribution of C_M to B is small, see Table I. The total theoretical shell correction is

$$C_T = C_K + C_{2s} + C_{2p} + C_M \tag{20}$$

and is shown for Al in Fig. 2.

A similar calculation of C was made by McGuire *et al.* [54], but was found to be inaccurate [55], see Fig. 2. The approximation given by Walske [14]

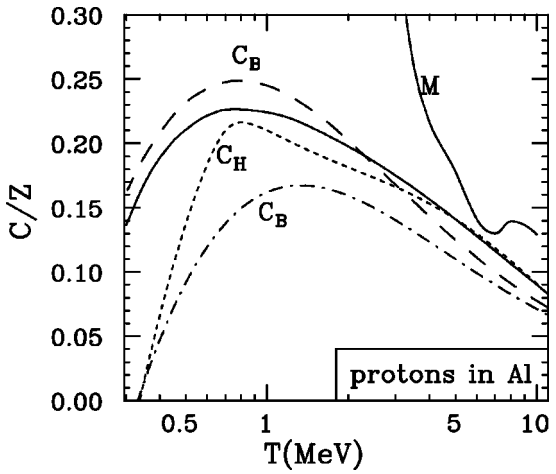

FIG. 2. The total shell correction for Al, $C_T = C_K + C_{2s} + C_{2p} + C_M$, Eq. (20), is shown by the solid line as a function of proton energy T. Functions calculated with the local plasma approximation LPA [36,60], Sec. III D, are also given. The dashed line C_B was calculated with the Lenz-Jensen potential of the atom with $\gamma = 1.336$ [44], the dash-dotted line was calculated with $\gamma = 2.06$, the value used in Sec. II C. The dotted line C_H was calculated with a Hartree-Fock-Slater potential [59]. The bulge of C_T and C_H at ~ 5 MeV is caused by the K-shell contribution, it does not appear for LPA functions calculated with a Thomas-Fermi or Lenz-Jensen potential. The function given by McGuire [54] is shown by the solid line M.

$$C_L = \frac{U}{\beta^2} + \frac{V}{\beta^4} \tag{21}$$

and discussed by Fano [2,3] is shown in Fig. 1.

D. Lindhard-Bonderup shell corrections

Major contributions to the theory of stopping power have been made by the Danish groups [1,36,45,56]. The study by Bonderup [36] using the local plasma approximation (LPA) is described briefly. It is a refinement of the calculations made for the electron gas by Lindhard and Winther [45]. Bonderup calculated the stopping number L using the radial electron density and the corresponding local plasma frequency obtained with the Lenz-Jensen potential, and derived the shell correction C_B. The parameter γ used in Eq. (6) is also used here. This function with $\gamma = 1.336$ was used by Shiomi-Tsuda *et al.* [44] to derive an I value for Al.[3] The function $C_B(\gamma = 1.336)$ is shown in Fig. 2 by the dashed line. For comparison, C_B calculated with $\gamma = 2.04$ used in Eq. (6) is shown by the dash-dotted line.

It has been suggested [58] that the use of, e.g., Hartree-Fock models of the atom to calculate the electron density would provide better agreement with experiments. Such a calculation, based on a potential derived from the Desclaux [59] atomic wave functions was made with a program described by Bichsel and Laulainen [60] and is shown by the dotted line C_H in Fig. 2. A shell structure is seen clearly but is more peaked than that seen in C_T.

Other aspects of the local plasma approximation were studied by Johnson and Inokuti [61]. They found that the oscillator strength spectra calculated with the local plasma approximation differed considerably from those obtained with the method described in the preceding section.

E. The scaling procedure

The corrections for different shells are similar in shape (Fig. 9 in Ref. [62], Fig. 1 in Ref. [21]). It thus appears plausible [63] to use a scaling procedure to obtain shell corrections for shells for which no calculations with Eqs. (17) and (18) have been made. For a shell ν, the procedure is defined by

$$C_\nu = V_\nu C_\mu(W_\mu, H_\nu \eta_\mu), \tag{22}$$

with $\eta_\mu = [\beta/(\alpha Z_{eff})]^2 = 18779\beta^2/Z_{eff}^2$ (Z_{eff} is the effective atomic central charge [14]), W_μ is the ionization potential for shell μ [21], and C_μ is known from calculations for a shell μ. Adjustable parameters V_ν and H_ν are introduced in order to fit experiments. As an example, the hydrogenic function [14] (dotted line in Fig. 1) scaled with $H_L = 1.2$ and $V_L = 1.17$ is shown in Fig. 1 by the dashed line. In previous studies the hydrogenic shell corrections [14,50] were used for this approach, and I values and the parameters H and V were determined by calculating least-squares fits to the experimental data, [3,20,21,42,48,64]. In Ref. [5], the Walske C_K and C_L were used, and C_M was scaled from C_L with $H_M = 12$, $V_M = 3/8$ for Al, $V_M = 4/8$ for Si. An extensive systematic study with this method was made by Janni [65]. The parameter sets thus derived were then used to extend calculations beyond the range of energies given in the experiments, and to interpolate for substances for which no experimental data are available, e.g., Refs. [65,5]. We can expect that good fits to experimental data can be obtained with a few parameters, but different sets of parameters will result from different experimental data sets [21]. Only calculations without free parameters will provide a test of the correctness of the theory of B and C. The present approach described in Sec. III C provides such a test.

IV. MEASUREMENT OF STOPPING POWER

Energy-loss spectra have been measured for particle beams in many cases [17,24,66–69]. A convenient way of characterizing $\phi(x,T,T_1)$ is to consider the moments [70] defined by

$$M_\nu = \int (T - T_1)^\nu \phi(x,T,T_1) dT_1 \Big/ \int \phi(x,T,T_1) dT_1. \tag{23}$$

[3]In principle, as Bonderup has emphasized [57], the I value and the shell corrections cannot be determined independently: $I/Z = \gamma K_J$, where $K_J = 7.583$ eV is the Bloch constant for the Lenz-Jensen model of the atom. Thus for Al, with the $\gamma = 1.336$ used in Ref. [44], I should be about 132 eV.

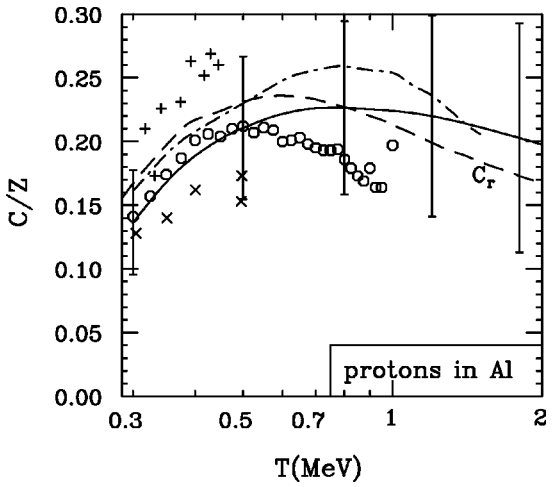

FIG. 3. Comparison of experimental shell corrections for protons with energies below 2 MeV in Al to the theoretical function C_T of Fig. 2 (solid line). A deviation of $\rho=\pm 3\%$ of L is shown by the vertical bars associated with C_T, see Sec. V A. The function C_r derived with Eq. (27) from the "reference stopping cross sections" of Paul *et al.* [79] (quoted uncertainty of $\sigma=\pm 0.7\%$) is given by the dashed line. The dash-dotted line gives the data by Luomajärvi [84], $\sigma=\pm 1.5\%$. Other experimental data are shown by the following symbols. ×, Semrad *et al.* [85], ±2%; ○, Santry and Werner [86], ±4%; +, Bednyakov *et al.* [87], ±2%.

The quantity M_1 is the mean energy loss $\langle\Delta\rangle=\langle T-T_1\rangle$ of the particles, while

$$\sigma_s^2=M_2-M_1^2 \tag{24}$$

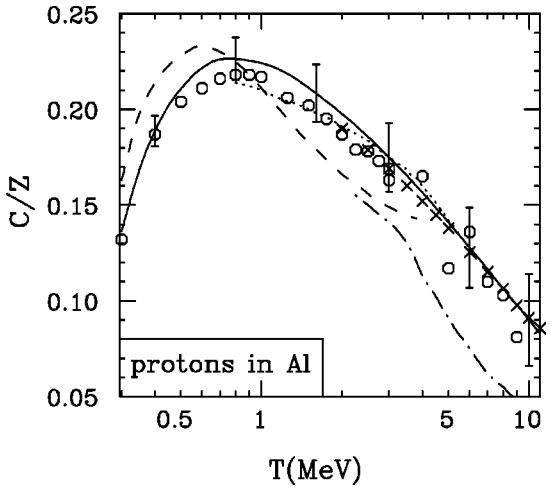

FIG. 4. Similar to Fig. 3 for T up to 11 MeV. The solid line represents C_T of Fig. 2. A deviation of $\rho=\pm 0.5\%$ of L is shown by the vertical bars associated with C_T. The dashed line represents Ref. [79]. The dotted line represents averaged experimental data from Andersen *et al.* [30] (quoted uncertainty of $\sigma=\pm 0.5\%$ for a single datum). The bulge in C_T at 5 MeV (Fig. 2) is seen in this function. The dash-dotted line gives results of Sørensen and Andersen [88], $\sigma=\pm 0.3\%$. Note that the Andersen-Ziegler tables [77] relied heavily on this reference, while Ref. [24] was not considered. ○, Shiomi-Tsuda *et al.* [44], $\sigma=\pm 0.35\%$; ×, Tschalär and Bichsel [24], $\sigma\sim\pm 0.3\%$.

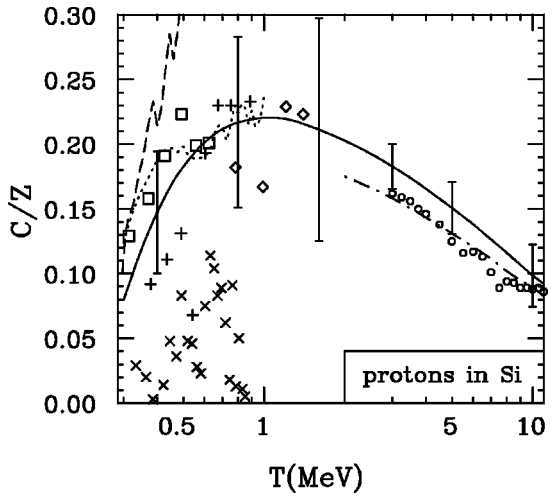

FIG. 5. Similar to Fig. 3 for experimental data for Si. The solid line represents C_T, Eq. (20). For $T<2$ MeV, deviations of $\rho=\pm 3\%$ of L, for $T>2$ MeV, $\rho=\pm 0.5\%$, are shown by the vertical bars associated with C_T. Dotted line, Santry and Werner [86], ±4%; dashed line, Khodyrev *et al.* [89], ±4.5%; dash-dotted line, Tschalär and Bichsel [24], $\sigma\sim\pm 0.3\%$; +, Carnera *et al.* [90], 8 points, ±2%; ◇, Melvin and Tombrello [91], 4 points, ±5%; □, Mertens and Bauer [92], 6 points, ±3%; ×, Izmailow *et al.* [93], 23 points, ±4.5%; o, Sakamoto [94], ±0.35%.

describes the width of $\phi(x,T,T_1)$. For very thin absorbers, $\phi(x,T,T_1)$ is strongly skewed [16,17]; for thick absorbers it begins to approach (but never reaches) a Gaussian shape [19,71], for which the full width at half maximum w_h would be given by $w_h=2.355\sigma_s$.

By defining the location of the maximum value of $\phi(x,T,T_1)$ as T_p, we call $\Delta_p=T-T_p$ the most probable

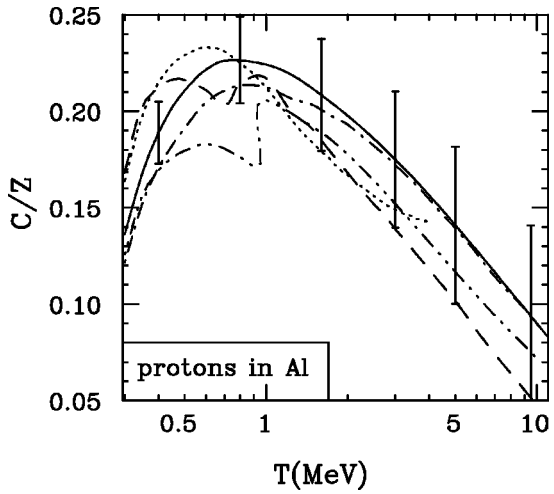

FIG. 6. Experimental shell corrections as a function of proton energy T derived from several stopping power tables for protons in Al. The solid line represents the current theory. A deviation of $\rho=\pm 1\%$ of L is shown by the vertical bars associated with C_T. The reference function from Paul *et al.* [79] is given by the dotted line. The ICRU function [5] is shown by the dash-dotted line, and that of Janni [65] by the dashed line. The Andersen-Ziegler function [77] is given by the dash-double-dotted line.

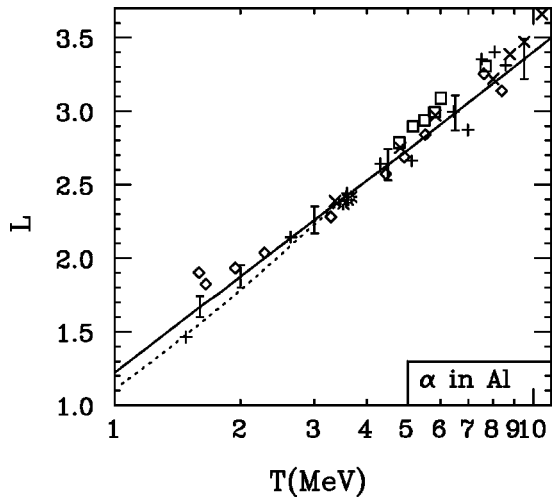

FIG. 7. Comparison of theoretical and experimental stopping numbers L for α particles in Al. The function $L(\beta)$ of Eq. (3), calculated with the C_T of Eq. (20) is given by the solid line. The vertical bars correspond to an uncertainty $\rho=\pm 4\%$ of L. An averaged experimental function L_x, Eq. (28), calculated with the tabulated values in ICRU [5] is given by the dotted line. The data by Andersen *et al.* [30] are not shown, they agree within 0.5% with the theoretical function. These data were used to derive L_1, Sec. II C. Some experimental data are given by the following symbols. +, Comfort *et al.* [95], $\pm 10\%$; $\diamond$, Nakata [96], $\pm 4.5\%$; $\square$, Santry and Werner [97], $\pm 4\%$; *, Desmarais and Duggan [98], $\pm 3\%$; $\times$, Räisänen *et al.* [99], $\pm 3\%$. The systematic deviation between the theory and the experiment below about 3 MeV could be explained by a reduced effective charge of the α particle.

energy loss [17]. In some measurements T_p has been used to characterize $\phi(x,T,T_1)$, and the quantity Δ_p/x was defined as the stopping power. This is an approximation to $\langle\Delta\rangle/x$. The calculation of Δ_p is more complex [17] than that of $\langle\Delta\rangle$, Eq. (1), and there is no simple correlation between the two.

Many issues here must be considered to get accurate results for S [24,44,72]. Among them are surface layers of heterogeneous materials (e.g., Al_2O_3 for Al), the escape of δ rays [73], the energy spectrum of the incident particles, increased energy loss due to multiple scattering [6,43], and losses due to ''nuclear collisions'' [1,5]. The nonlinearity of the system used to measure T_1 must be known [17,30,74,75]. All particles, except those that made nuclear reactions, must be included in $\phi(x,T,T_1)$ for the calculation of M_ν.

When a particle beam of initial energy T_0 traverses an absorber, the change of $S(T)$ with decreasing energy must be taken into account [19,26]. This is done with the ''range equation.'' After a thickness x, the residual mean energy T_r, in the continuous-slowing-down approximation, is defined by

$$x(T_0,T_r)=\int_{T_r}^{T_0}\frac{1}{S(T)}dT. \tag{25}$$

If $\langle\Delta\rangle=T_0-T_r$ is small compared to T_0, the stopping power for the energy $(T_0+T_r)/2$ is

$$S=\frac{\langle\Delta\rangle}{x}, \tag{26}$$

otherwise, a suitable function must be chosen for $S(T)$ and measured values of x are compared to $x(T_0,T_r)$ [24]. The same approach is used for total ranges, defined by $R(T_0)=x(T_0,T_l)$, where $T_l\sim 0$ [48,66,67,76]. Note that the lower limit T_l of the integral may not be well defined. In some measurements it will be given by the sensitivity of the range detector, e.g., Refs. [42,48]. In principle, for a proton beam, the H atom formed at the end of the range could diffuse through the absorber for an indefinite path length.

The absorber thickness x is expressed either as a length (cm, mm, μm, nm) or as a surface density $x\rho$ (g/cm^2) where ρ is the density of the absorber. Frequently the energy loss (eV) per 10^{15} atoms/cm^2 is given, with a factor $q=602.2/A$ (A is the atomic weight of the absorber in g) for conversion to MeV cm^2/g [77].

V. COMPARISON OF THEORY AND EXPERIMENT

The values of S change by a factor of 10 for $0.3<T(\mathrm{MeV})<10$. Thus a graphical representation of the $S(T)$ data does not show much detail, e.g., Refs. [9,77]. ''Extracted'' functions can be used [3] to show differences between data sets more clearly. Here, ''experimental shell corrections'' are derived from the experimental data for S. They are defined next.

A. Calculation of experimental shell corrections and errors

An experimental shell correction C_x can be calculated from a given experimental stopping power $S_x(\beta)$ by rewriting Eq. (3) as

$$C_x(\beta)/Z=f(\beta)-\ln I+zL_1(\beta)+L_2(z)-L_x, \tag{27}$$

where

$$L_x=\beta^2 S_x(\beta)A/(0.307\,08z^2Z) \tag{28}$$

is the experimental value of L_x, derived from Eq. (1). The quantity C_x is similar to the quantity $X=f(\beta)-L_x$ defined in NAS-NRC Publication 1133 [3], but at that time I was not well known, the Barkas correction had not yet been discerned and L_2 was disregarded (see Figs. 1 and 2 in Ref. [20]).

Clearly, C_x will depend on the assumptions about L_1, L_2, the I value, and the corrections discussed in Sec. II D, but any changes in these functions will have the same effect for all experimental data sets $S_x(\beta)$. In other words, differences in $C_x(\beta)$ for data from different sources will not be due to these assumptions, but will be representative of the experimental uncertainties.

Instead of showing in the figures the uncertainties σ given by the authors for their experiments, error bars are associated to the theoretical functions C_T. They are given by a fraction ρ of $L(\beta)$ in Eq. (3). The authors' estimates of σ are given in the figure captions.

TABLE II. Stopping power S and range R calculated with the present theory for protons with energy T (MeV). The function S(Al) differs from Ref. [5] by 0.5% at 0.3 MeV, −0.2% at 1 MeV and −0.17% at 3 MeV. For Si, the differences are 2.3% at 0.3 MeV, −0.4% at 1 MeV, and −0.15% at 3 MeV. This is mainly due to differences in the I values. For R, an initial range at 0.3 MeV from Ref. [5] is used. The effect of nuclear collisions is not included, it can be found in Ref. [5]. Multiple scattering corrections will depend on the method of measurement. Columns 2 and 4 are in MeV cm^2/g, column 5 in keV/μm, columns 3 and 6 are in mg/cm^2, and column 7 is in μm.

T	S(Al)	R(Al)	S(Si)	S_μ(Si)	R(Si)	R_μ(Si)
0.3	318.11	0.800	323.59	75.365	0.74	3.18
0.4	281.10	1.118	284.29	66.212	1.05	4.52
0.5	252.10	1.482	255.28	59.455	1.41	6.06
0.6	229.43	1.888	231.75	53.976	1.81	7.78
0.7	210.86	2.335	213.15	49.643	2.25	9.67
0.8	195.46	2.821	197.69	46.042	2.73	11.73
0.9	182.37	3.344	184.58	42.988	3.25	13.95
1.0	171.09	3.904	173.27	40.355	3.80	16.32
1.2	152.69	5.131	154.84	36.062	5.01	21.51
1.4	138.36	6.497	140.43	32.705	6.36	27.29
1.6	126.84	7.997	128.78	29.992	7.83	33.62
1.8	117.30	9.626	119.18	27.757	9.43	40.51
2.0	109.24	11.383	111.06	25.866	11.16	47.92
2.5	93.67	16.316	95.34	22.205	16.00	68.71
3.0	82.39	21.995	83.93	19.547	21.57	92.61
3.5	73.79	28.393	75.21	17.518	27.84	119.53
4.0	66.99	35.488	68.33	15.914	34.78	149.36
4.5	61.47	43.261	62.72	14.609	42.39	182.02
5.0	56.89	51.699	58.06	13.523	50.65	217.47
6.0	49.68	70.512	50.74	11.817	69.04	296.46
7.0	44.26	91.834	45.22	10.533	89.89	385.96
8.0	40.01	115.591	40.90	9.526	113.11	485.65
9.0	36.58	141.722	37.41	8.713	138.64	595.27
10.0	33.75	170.176	34.53	8.042	166.43	714.60
11.0	31.37	200.908	32.10	7.476	196.44	843.46
12.0	29.33	233.878	30.04	6.996	228.63	981.67
13.0	27.56	269.048	28.24	6.577	262.96	1129.08
14.0	26.02	306.386	26.66	6.210	299.40	1285.55
15.0	24.66	345.861	25.27	5.885	337.92	1450.94
16.0	23.45	387.446	24.03	5.597	378.50	1625.16
18.0	21.38	476.847	21.92	5.105	465.71	1999.60
20.0	19.68	574.401	20.19	4.701	560.85	2408.10
22.0	18.26	679.942	18.73	4.363	663.75	2849.94
24.0	17.05	793.317	17.50	4.075	774.27	3324.49
26.0	16.01	914.385	16.43	3.827	892.28	3831.17
28.0	15.10	1043.022	15.50	3.610	1017.64	4369.44
30.0	14.31	1179.106	14.68	3.420	1150.24	4938.79

B. Comparison of calculated and experimental shell corrections for protons

The derivation of parameters for theories of S has a long history [12,3], as have compilations of experimental data [3,6,5,9,78,77,65,20,79,21,80–82]. Therefore, there is no need to compare the present theory with *all* experimental data: the scatter of the data will be similar to that seen in the compilations. Shell corrections C_x derived from experiments for protons in Al are shown in Figs. 3 and 4. In general, the C_x agree with the theoretical function derived here within experimental uncertainties σ given by the authors. ''Reference cross sections'' based on a statistical analysis of *all* available data were given by Paul *et al.* [79]. The function $C_r(T)$ derived from this function is given by the dashed line in Figs. 3 and 4. $C_r(T)$ agrees with C_T to within 1σ for $T > 0.6$ MeV, but differs by as much as 2.3σ at 0.4 MeV. Other experimental data mostly agree with C_T to within 1σ. Most of the data available for Si are shown in Fig. 5. The

TABLE III. Stopping power S and range R calculated with the present theory for α particles with energy T (MeV). The function S(Al) differs from Ref. [5] by 13% at 1 MeV, 1.7% at 3 MeV, and 0.1% at 5 MeV, see Fig. 7. For Si, the differences are 9.6% at 1 MeV, 0.7% at 3 MeV, and -0.1% at 5 MeV. For R, an initial range at $T=4$ MeV from Ref. [5] is used. The effect of nuclear collisions is not included, it can be found in Ref. [5]. Multiple scattering corrections will depend on the method of measurement. Columns 2 and 4 are in MeV cm^2/g, column 5 in keV/μm, columns 3 and 6 are in mg/cm^2, column 7 in μm.

T	S(Al)	R(Al)	S(Si)	S_μ(Si)	R(Si)	R_μ(Si)
1.0	1347.23		1330.41	309.852		
1.2	1282.70		1270.90	295.992		
1.4	1215.36		1205.11	280.670		
1.6	1151.94		1141.39	265.830		
1.8	1086.85		1085.55	252.823		
2.0	1035.18		1036.02	241.289		
2.2	987.03		984.23	229.227		
2.4	942.70		942.04	219.402		
2.6	902.27		903.28	210.374		
2.8	865.40		867.68	202.083		
3.0	831.68		834.92	194.454		
3.5	758.59		763.55	177.832		
4.0	698.08	4.283	704.14	163.995	4.14	17.78
4.5	647.42	5.020	654.17	152.357	4.87	20.91
5.0	604.05	5.813	611.63	142.450	5.65	24.27
5.5	567.82	6.659	574.97	133.909	6.49	27.86
6.0	536.13	7.559	542.67	126.388	7.38	31.67
6.5	508.15	8.510	514.86	119.911	8.31	35.70
7.0	483.26	9.512	490.03	114.128	9.30	39.94
8.0	440.86	11.667	447.61	104.248	11.42	49.05
9.0	406.05	14.019	412.67	96.111	13.73	58.97
10.0	376.92	16.563	383.38	89.288	16.23	69.70
11.0	352.17	19.296	358.42	83.476	18.92	81.22
12.0	330.83	22.214	336.88	78.459	21.78	93.50
13.0	312.22	25.313	318.07	74.078	24.82	106.55
14.0	295.84	28.592	301.49	70.218	28.03	120.34
15.0	281.30	32.046	286.78	66.790	31.41	134.87
16.0	268.29	35.674	273.60	63.721	34.96	150.12
18.0	245.95	43.443	250.95	58.445	42.57	182.77
20.0	227.44	51.881	232.15	54.067	50.82	218.22
22.0	211.81	60.976	216.26	50.367	59.72	256.41
24.0	198.41	70.715	202.65	47.196	69.24	297.30
26.0	186.79	81.086	190.85	44.448	79.38	340.84
28.0	176.61	92.080	180.49	42.036	90.13	386.98
30.0	167.62	103.687	171.32	39.901	101.47	435.68

only conclusion drawn from the figure is that there is no disagreement with C_T.

The diversity of the various algorithms used for the production of tables can be seen in Fig. 6 for Al. The functions C_x were calculated with Eq. (27) from the data tables given in the references. The variations seen are due in part to the use of different sets of experimental data for the parameter searches, and in part due to different assumptions about the algorithms. The values of C_x for $T>1$ MeV agree to 1% of L or better with C_T. The change in algorithms used below 1 MeV produces the irregularities seen in the figure. For Si, the functions are similar. Measurements made with Si detectors to determine straggling functions [83] also provided stopping powers. Most of the experimental values agreed within $\pm 1\%$ with calculated S, but no complete evaluation was made except for $T\sim 40$ MeV [17].

C. Experimental data for α particles

Experimental S for α particles at $T=1$ MeV differ by about 10% for Al, 3% for Si from S calculated with Eqs. (1)–(3). Instead of comparing shell corrections, the functions L of Eqs. (3) and (28) are compared in Fig. 7. The solid line shows the present theory and the dashed line the function of Ref. [5]. In addition, all experimental data for $T>2.5$ MeV and a few values below 2.5 MeV are shown. The

increasing difference between L_x and L with decreasing T could be caused by an error due to the extrapolation of L_1, Eq. (6), to lower energies, a reduction of the effective charge of the α particle or effects not yet discerned. An uncertainty of L_x at 1 MeV of about $\pm 4\%$ would encompass most experimental data. Note that the data in Ref. [30] have been used in the derivation of L_1 [31] and therefore these α data will agree with current theory as well as the proton data in Fig. 4.

VI. CONCLUSIONS

An extension of the calculations with Eqs. (17) and (18) to $T>10$ MeV or $E>2500$ Ry is unwieldy. Since the shell corrections amount to 2% at $T=10$ MeV, an extension to larger T with the scaled hydrogenic approximation will introduce negligible errors into calculations of S, Fig. 1. This has been done for the calculation of Tables II and III.

The theory for C presented here contains no free parameters and agrees with the experimental data within experimental uncertainties. For $T<0.8$ MeV, the uncertainty in L_1 due to the extrapolation permits no conclusion about the validity of C_T.

In order to further test the present theory, much more accurate experiments would be needed. A similar situation has been found for straggling in Si [17]. From the experimental data seen in Fig. 3 for protons, it appears hopeless to extract experimental values for the electron capture and loss effect, but from the Nara data in Fig. 4, the effect would appear to be quite small even at 0.3 MeV if the extrapolation of L_1 is appropriate. For α particles, the systematic deviation between the experimental data and the current theory seen in Fig. 7 must be explored further.

I dare suggest that at this time theoretical calculations based on the GOS discussed here will be more accurate for small to intermediate Z than most of the existing measurements for proton energies below about 4 MeV. The I values could be obtained from measurements at higher energies, e.g., Refs. [19,26].

If it is assumed that I is correct, the accuracy of the functions is about $\pm 3\%$ at 0.3 MeV/u, 0.5% at 1 MeV/u, and 0.3% above 10 MeV/u. For $z \geqslant 2$, charge state corrections may be needed [31].

ACKNOWLEDGMENTS

I am grateful to the people in the references with most of whom I discussed various aspects of this study over the last 50 years. Special thanks are due to Dr. M. Inokuti for his suggestions about improving the manuscript, and Professor H. Paul in Linz for providing me with his lists of experimental data. Support by the Greenwalt family foundation is greatly appreciated.

[1] N. Bohr, K. Dan. Vidensk. Selsk. Mat. Fys. Medd. **18**, 8 (1948).
[2] U. Fano, Annu. Rev. Nucl. Sci. **13**, 1 (1963).
[3] U. Fano, Nat. Acad. Sci.-Nat. Res. Council Report No. 1133, 1964 (unpublished).
[4] M. Inokuti, Rev. Mod. Phys. **43**, 297 (1971); **50**, 23 (1978).
[5] International Commission on Radiation Units Report No. 49 (unpublished), ICRU, 7910 Woodmont Ave., Bethesda, MD 20814.
[6] H. Bichsel, *Passage of Charged Particles, Through Matter*, 3rd ed., edited by D. E. Gray (McGraw-Hill, New York, 1972), p. 8-142.
[7] H. Bichsel, J. Chim. Phys. Phys.-Chim. Biol. **90**, 617 (1993).
[8] H. Bichsel, *Charged Particle-Matter Interactions*, edited by G.W.F. Drake (AIP, Woodbury, NY, 1996), p. 1032.
[9] J.F. Ziegler, J. Appl. Phys. **85**, 1249 (1999).
[10] H. Bethe, Ann. Phys. (Leipzig) **5**, 325 (1930); Z. Phys. **76**, 293 (1932).
[11] H. Bethe, in *Handbuch der Physik*, edited by A. Smekal (Springer, Berlin, 1933), Vol. XXIV/1, Chap. 3.
[12] M.S. Livingston and H.A. Bethe, Rev. Mod. Phys. **9**, 245 (1937).
[13] F. Bloch, Ann. Phys. (Leipzig) **16**, 285 (1933).
[14] M.C. Walske, Phys. Rev. **88**, 1283 (1952); **101**, 940 (1956).
[15] W.H. Barkas, J. N. Dyer, and H. H. Heckman Phys. Rev. Lett. **11**, 26 (1963).
[16] H. Bichsel and R.P. Saxon, Phys. Rev. A **11**, 1286 (1975).
[17] H. Bichsel, Rev. Mod. Phys. **60**, 663 (1988).
[18] H. Bichsel, Nucl. Instrum. Methods Phys. Res. B **52**, 136 (1990).
[19] H. Bichsel and T. Hiraoka, Int. J. Quantum Chem., Quantum Chem. Symp. **23**, 565 (1989).
[20] H. Bichsel and L.E. Porter, Phys. Rev. A **25**, 2499 (1982).
[21] H. Bichsel, Phys. Rev. A **46**, 5761 (1992).
[22] J. D. Jackson, *Classical Electrodynamics* (Wiley, New York, 1962), Chap. 13.
[23] E. Shiles, T. Sasaki, M. Inokuti, and D.Y. Smith, Phys. Rev. B **22**, 1612 (1980).
[24] C. Tschalär and H. Bichsel, Phys. Rev. **175**, 476 (1968); C. Tschalär, Ph.D. dissertation, University of Southern California, 1967.
[25] H. Bichsel and T. Hiraoka, Nucl. Instrum. Methods Phys. Res. B **66**, 345 (1992).
[26] H. Bichsel, T. Hiraoka, and K. Omata, Radiat. Res. **153**, 208 (2000).
[27] J. Lindhard and A.H. Sørensen, Phys. Rev. A **53**, 2443 (1996).
[28] A.H. Sørensen, Phys. Rev. A **55**, 2896 (1997).
[29] J.A. Golovchenko, D.E. Cox, and A.N. Goland, Phys. Rev. B **26**, 2335 (1982).
[30] H.H. Andersen, J.F. Bak, H. Knudsen, and B.R. Nielsen, Phys. Rev. A **16**, 1929 (1977).
[31] H. Bichsel, Phys. Rev. A **41**, 3642 (1990).
[32] J. Lindhard, Nucl. Instrum. Methods **132**, 1 (1976).
[33] J.C. Ashley, R.H. Ritchie, and W. Brandt, Phys. Rev. B **5**, 2393 (1972).
[34] G. Basbas, Nucl. Instrum. Methods Phys. Res. B **4**, 227 (1984).

[35] L.H. Andersen *et al.*, Phys. Rev. Lett. **62**, 1731 (1989).
[36] E. Bonderup, K. Dan. Vidensk. Selsk. Mat. Fys. Medd. **35**, 17 (1967).
[37] L.E. Porter, Nucl. Instrum. Methods Phys. Res. B **149**, 373 (1999).
[38] S.P. Ahlen, Rev. Mod. Phys. **52**, 121 (1980).
[39] B.S. Yarlagadda, J.E. Robinson, and W. Brandt, Phys. Rev. B **17**, 3473 (1978).
[40] E. Fermi, Phys. Rev. **57**, 485 (1940).
[41] R.M. Sternheimer, M.J. Berger, and S.M. Seltzer, At. Data Nucl. Data Tables **30**, 261 (1984).
[42] H. Bichsel and E.A. Uehling, Phys. Rev. **119**, 1670 (1960).
[43] C. Tschalär and H. Bichsel, Nucl. Instrum. Methods **62**, 208 (1968).
[44] N. Shiomi-Tsuda, N. Sakamoto, H. Ogawa, and U. Kitoba, Nucl. Instrum. Methods Phys. Res. B **159**, 123 (1999).
[45] J. Lindhard and A. Winther, K. Dan. Vidensk. Selsk. Mat. Fys. Medd. **34**, 4 (1964).
[46] P. Sigmund and U. Haagerup, Phys. Rev. A **34**, 892 (1986).
[47] J.M. Peek, Phys. Rev. A **27**, 2384 (1983).
[48] H. Bichsel, R.F. Mozley, and W.A. Aron, Phys. Rev. **105**, 1788 (1957).
[49] K. Sera, K. Ishii, A. Yamadera, A. Kuwako, M. Kamiya, M. Sebata, S. Morita, and T.C. Chu, Phys. Rev. A **22**, 2536 (1980).
[50] H. Bichsel, Phys. Rev. A **28**, 1147 (1983).
[51] S.T. Manson, Phys. Rev. **6**, 1013 (1972).
[52] F. Herman and S. Skillman, *Atomic Structure Calculations* (Prentice-Hall, Englewood Cliffs, NJ, 1963).
[53] W. H. Press *et al.*, *Numerical Recipes* (Cambridge University Press, Cambridge, England, 1986).
[54] E.J. McGuire, Phys. Rev. A **28**, 49 (1983); **28**, 53 (1983).
[55] H. Bichsel, M. Inokuti, and D.Y. Smith, Phys. Rev. A **33**, 3567 (1986).
[56] J. Lindhard, M. Scharff, and H.E. Schiøtt, K. Dan. Vidensk. Selsk. Mat. Fys. Medd. **33**, 14 (1963).
[57] E. Bonderup (private communication).
[58] W.K. Chu and D. Powers, Phys. Lett. **40A**, 23 (1972).
[59] J.P. Desclaux, Comput. Phys. Commun. **9**, 31 (1975).
[60] H. Bichsel and N.S. Laulainen, Bull. Am. Phys. Soc. **16**, 842 (1971).
[61] R.E. Johnson and M. Inokuti, Comments At. Mol. Phys. **14**, 19 (1983).
[62] *Radiation Dosimetry*, edited by F.H. Attix and Wm. C. Roesch (Academic Press, New York, 1968), Chap. 4.
[63] J.O. Hirschfelder and J.L. Magee, Phys. Rev. **73**, 207 (1948).
[64] International Commission on Radiation Units Report No. 37, 1984 (unpublished), ICRU, 7910 Woodmont Ave., Bethesda, MD 20814.
[65] J.F. Janni, At. Data Nucl. Data Tables **27**, 147 (1982).
[66] D.B. Parkinson, R.G. Herb, J.C. Bellamy, and C.M. Hudson, Phys. Rev. **52**, 75 (1937).
[67] R.R. Wilson, Phys. Rev. **60**, 749 (1941).
[68] H.A. Wilcox, Phys. Rev. **74**, 1743 (1948) is given as an early example of the direct measurement of *S*; note that most probable energy losses were determined.
[69] P.D. Bourland, W.K. Chu, and D. Powers, Phys. Rev. B **3**, 3625 (1971).
[70] U. Fano, Phys. Rev. **92**, 328 (1953).
[71] C. Tschalär, Nucl. Instrum. Methods **61**, 141 (1968); **64**, 237 (1969).
[72] H.H. Andersen, P. Hornshøj, L. Højsholt-Poulsen, H. Knudsen, B.R. Nielsen, and R. Stensgaard, Nucl. Instrum. Methods **136**, 119 (1976).
[73] N. Laulainen and H. Bichsel, Nucl. Instrum. Methods **104**, 531 (1972).
[74] C.C. Hanke and H. Bichsel, K. Dan. Vidensk. Selsk. Mat. Fys. Medd. **38**, 3 (1970).
[75] International Commission on Radiation Units Report No. 31, 1979 (unpublished).
[76] R. Mather and E. Segrè, Phys. Rev. **84**, 191 (1951); H. Bichsel, *ibid.* **120**, 1012 (1960).
[77] H.A. Andersen and J.F. Ziegler, *Hydrogen Stopping Power and Ranges in all Elements* (Pergamon Press, New York, 1977).
[78] W. Whaling, in *Encyclopedia of Physics*, edited by S Flügge (Springer-Verlag, Berlin, 1958), Vol. XXXIV.
[79] H. Paul, D. Semrad, and A. Seilinger, Nucl. Instrum. Methods Phys. Res. B **61**, 261 (1991).
[80] F. Hubert, R. Bimbot, and H. Gauvin, At. Data Nucl. Data Tables **46**, 1 (1990); see also P. Sigmund, Phys. Rev. A **56**, 3781 (1997).
[81] Int. Atomic Energy Agency Report No. IAEA-TECDOC-799, 1995 (unpublished).
[82] H. Paul (unpublished), at the web site: www.exphys.uni-linz.ac.at/stopping
[83] J.J. Kolata, T.M. Amos, and H. Bichsel, Phys. Rev. **176**, 484 (1968).
[84] M. Luomajärvi, Radiat. Eff. **40**, 173 (1979).
[85] D. Semrad, P. Mertens, and P. Bauer, Nucl. Instrum. Methods Phys. Res. B **15**, 86 (1986); Rev. Sci. Instrum. **57**, 1368 (1986).
[86] D.C. Santry and R.D. Werner, Nucl. Instrum. Methods **185**, 517 (1981); **188**, 211 (1981).
[87] A.A. Bednyakov, Yu.V. Bulgakov, V.S. Nikolaev, and V.L. Chernov, Zh. Eksp. Teor. Fiz **78**, 1900 (1980) [Sov. Phys. JETP **51**, 954 (1980)].
[88] H. Sørensen and H.H. Andersen, Phys. Rev. B **8**, 1854 (1973).
[89] V.A. Khodyrev, V.N. Mizgulin, E.I. Sirotonin, and A.F. Tulinov, Radiat. Eff. **83**, 21 (1984).
[90] A. Carnera, G. Della Mea, A.V. Drigo, S. Lo Russo, P. Mazzoldi, and G.G. Bentini, Phys. Rev. B **17**, 3492 (1978).
[91] J.D. Melvin and T.A. Tombrello, Radiat. Eff. **26**, 113 (1975).
[92] P. Mertens and P. Bauer, Nucl. Instrum. Methods Phys. Res. B **33**, 133 (1988).
[93] Sh.Z. Izmailow, E.I. Sirotonin, and A.F. Tulinov, Nucl. Instrum. Methods **168**, 81 (1980).
[94] N. Sakamoto (private communication).
[95] J.R. Comfort, J.F. Decker, E.T. Lynk, M.O. Scully, and A.R. Quinton, Phys. Rev. **150**, 249 (1966).
[96] H. Nakata, Can. J. Phys. **47**, 2545 (1969).
[97] D.C. Santry and R.D. Werner, Nucl. Instrum. Methods Phys. Res. B **1**, 13 (1984); **5**, 449 (1984).
[98] D. Desmarais and J.L. Duggan, Am. J. Phys. **52**, 408 (1984).
[99] J. Räisänen *et al.*, Radiat. Eff. Defects Solids **118**, 2 (1991).